CD137 deficiency causes immune dysregulation with predisposition to lymphomagenesis

Supplementary Appendix

Table of Contents

Supplementary Patient Clinical Histories

Supplementary Materials and Methods

Supplementary References

Supplementary Tables and Figures

Supplementary Patient Clinical Histories

Patient 1 (AII-1, Fig. 1A) was born to consanguineous Turkish parents, presented with Burkitt's lymphoma (Fig. 1B) at 2 years of age. A lobulated mass in the small intestine was observed (Fig. 1B). Subsequent imaging demonstrated renal and hepatic metastases (Fig. 1B, Fig. S1A), and a lesion in the right para-spinal area infiltrating the adjacent para-vertebral muscle (Fig. S1A). The patient was treated according to the NHL BFM 2000 treatment regimen, including cytoreductive prophase treatment with cyclophosphamide, dexamethasone, and intravenous methotrexate (block AA, BB and CC). Rituximab treatment was initiated due to CD20 positivity. A reduction in tumor size was observed and the patient is currently in remission at the age of 3 years. He also suffered from recurrent ear infections, hepatosplenomegaly and hypogammaglobulinemia (Tables 1 and S1). The patient has a 7-year old sibling (AII-2, Fig. 1A) without obvious clinical phenotype and no family history of immunodeficiency.

Patient 2 (BII-1, Fig. 1A) was born to consanguineous Palestinian parents. He first presented with recurrent episodes of pneumonia (Fig. S1B) during the first 3 years of life. Bi-lateral ground glass opacities indicative of a chronic lung disease were subsequently demonstrated (Fig. S1C). He displayed autoimmune lymphoproliferative syndrome (ALPS)-like disease manifestations at the age of 6 years. Hepatosplenomegaly (Fig. S1D) and lymphadenopathy (Fig. S1E, S1F, S1G) were noted in physical examination and signs of autoimmunity including autoimmune hemolytic anemia (AIHA) and immune thrombocytopenic purpura (ITP) along with positive anti-nuclear antibodies (ANA) were detected (Tables 1 and S1). An Epstein-Barr virus (EBV)-related lymphoproliferative disorder with a monoclonal T-cell population was demonstrated in lymph node pathology (Fig. S1H) which was EBER positive (Fig. S1I). The patient was treated with sirolimus and glucocorticoids which he responded well to. Cellcept therapy has recently been initiated due to persistence of

autoimmune features (i.e. AIHA, ITP, ANA positivity) upon tapering of glucocorticoid treatment. Co-trimoxazole antibiotic prophylaxis is routinely administered as well. The patient has two siblings (BII-2, Fig. 1A) without overt clinical symptoms and no family history of immunodeficiency.

Patient 3 (CII-2, Fig. 1A), a boy born to consanguineous Turkish parents, manifested with herpes labialis and a lower respiratory tract infection at the age of six years. Hepatosplenomegaly (Fig. S1J) and lymphadenopathy were found during physical examination. Episodes of pneumonia, recurrent tonsillitis, otitis media and chronic suppurative otitis media were noted since the age of eight years (Table 1). Additional features included atopic dermatitis and xerosis. Laboratory evaluation revealed a positive direct Coombs test and hypergammaglobulinemia (Table S1), necessitating IVIG substitution therapy. At ten years of age, the patient was evaluated due to diffuse lymphadenopathy (bilateral cervical, submandibular and axillary nodes). An infectious etiology was ruled out. Submandibular lymph node biopsy exhibited large, prominent, multinucleated Reed-Sternberg cells (Fig. 1B) with EBER-positive lymph node histopathology (Fig. 1C). Immunohistochemistry showed weak CD20 staining and positive CD30 staining. Non-malignant nodular splenic lesions were observed, associated with lymphoproliferation. A diagnosis of Hodgkin lymphoma, stage 1, was established and the patient was treated according to GPOH-HD 95 therapy protocol, including two cycles of chemotherapy with adriamycin, vincristine, etoposide and prednisone. He is currently in remission. He is treated with immunoglobulin substitution and amoxicillin prophylaxis (Table 1). The patient has one sibling who is currently 14 years old (CII-1, Fig. 1A). She experienced recurrent tonsillitis until the age of ten years. Immunoglobulin levels were slightly elevated. Other than that, the patient has no remarkable family history of immunodeficiency.

Patient 4 (DII-2, Fig. 1A), a 33 year old male was born to non-consanguineous Colombian parents, presented with recurrent otitis media and sinusitis since the age of

eight. Between the age of 20-22 years, five episodes of pneumonia were documented. Laboratory workup revealed decreased serum IgG, IgM and IgA (Table S1) and no detectable IgG serum antibodies against rubella. The presumptive diagnosis of CVID was established and IVIG replacement therapy was initiated (Table 1). During the following 3 years, the patient was hospitalized with granulomatous pleuropneumonia, while *H. pylori* erythematous gastritis and chronic sinusitis (Fig. S1K) were noted. The patient has one healthy 32 year old sibling (DII-1, Fig. 1A). She suffered from recurrent infections during childhood. No family history of immunodeficiency is otherwise known.

Supplementary Materials and Methods

Study Subjects

All procedures were performed upon informed consent and assent from patients, first-degree relatives, and healthy donor controls in accordance with the ethical standards of the institutional and/or national research committees and with the current update of the Declaration of Helsinki.

Genetic Analysis

Whole-exome sequencing was performed to determine the underlying genetic defect in *TNFRSF9* in all four patients. Genomic DNA was isolated from whole blood of patients and their first-degree relatives for generation of whole-exome libraries using the SureSelect XT Human All Exon V5+UTR or V6+UTR kit (Agilent Technologies, USA). Barcoded libraries were sequenced on a NextSeq 500 platform (Illumina, USA) with an average coverage depth of 100x. Bioinformatics analysis and subsequent filtering identified rare sequence variants. *TNFRSF9*/*CD137* mutations were confirmed by Sanger sequencing.

In silico analysis of the exon 2: c.100+1G>A substitution was performed with the bioinformatics tools NetGene2 (http://www.cbs.dtu.dk/services/NetGene2/) and

Fruitfly (http://www.fruitfly.org/seq_tools/splice.html). These tools predicted that the mutation affected the donor splice site at the end of exon 2. Moreover, multiple alignments of DNA sequences of *CD137* orthologous from several species show that exon2: c.100 +1G is a highly conserved region. We used the SIFT, PolyPhen-2 and CADD algorithms to assess these *in silico*[1].

Expansion of T cells

Patient or control blood was subjected to a Ficoll density gradient centrifugation, after which peripheral blood mononuclear cells (PBMCs) were collected from the interface. T cells were expanded by stimulation of the PBMCs with irradiated feeder cells (PBMCs from healthy donors), PHA (1µg/ml) and IL-2 (100U/mL) in RPMI medium containing 5% human serum. Cell lines were tested negative for mycoplasma by PCR using VenorGeM Mycoplasma Detection Kit (MP0025, Sigma-Aldrich).

Flow Cytometry

For analysis of cell surface markers, PBMCs were used as starting material or 100 µl of whole blood in EDTA was lysed using RBC Lysis Buffer (eBioscience). Cells were washed twice in FACS buffer (PBS with 5% FBS), and resuspended in 100 µl of FACS buffer with antibodies for 30 min on ice. Cells were washed twice in FACS buffer, resuspended in 300 µl of FACS buffer.

Western Blot

Whole cell lysates were prepared from control- and patient-derived expanded T cells or B-LCLs, loaded on 10% polyacrylamide TRIS-HEPES-SDS gel and separated by SDS-PAGE. Proteins were transferred to polyvinylidene difluoride (PVDF) membrane using iBlot system (Invitrogen). Blots were probed overnight with 1:1000 dilution of specific antibodies, and 1:8000 dilution of anti-HSP90α/β (Santa

Cruz) as a loading control. Bands were revealed using Amersham ECL Select Western Blotting Detection Reagent (GE Healthcare).

T- and B-cell stimulation

PBMCs were labeled with either CellTrace Violet Cell Proliferation dye VPD450 (ThermoFisher) or CFSE 5µM (ThermoFischer), washed with PBS with 10% FCS in a ratio of 1:1. Labeled PBMCs were stimulated with anti-CD3-coupled beads (Bio-anti-CD3, OKT3 from eBioscience coupled with anti-Biotin MACSiBeads from Miltenyi Biotec) at a ratio of 10:1 with and without 1 µg ml^{-1} soluble anti-CD28 (CD28.2, eBioscience) or anti-CD3 with anti-CD137, 10 µg/ml (R&D Systems) or CD137L, 20 ng/ml (R&D Systems) and stained for cell surface markers. For blocking experiments of CD137 in T cells, a neutralizing anti-CD137 monoclonal antibody (BBK-2 clone, Invitrogen) was added at increasing concentrations (1-2µg/mL) or mouse IgG1, kappa isotype control P3.6.2.8.1 (Invitrogen) to anti-CD3-coupled beads and stained for cell surface markers. For B-cell proliferation assays PBMCs were stimulated with CpG ODN 2006, 50nM (ODN7909, Invivogen), or CD40 ligand 200ng/ml (R&D Systems) in combination with rhIL4 100 ng/ml, rhIL21 20ng/ml (R&D Systems) or anti-IgM 20µg/ml (Southern Biotech). For sorting of CD3 T cells and naïve B cells, PBMCs were stained for CD3, CD19, CD27 and IgD: PE-CY7 anti-CD3 (Beckman Coulter), PerCP/Cy5.5 anti-CD19 (HIB19, Biolegend), BV480 anti-IgD (IA6-2, BD), PE anti-CD27 (L128, BD), and afterwards sorted by FACS for $CD3^+$, $CD19^+CD27^-IgD^+$ or $CD19^+CD27^+$ populations, respectively. Sorted PBMCs were then labeled with either CellTrace Violet Cell Proliferation dye VPD450 (ThermoFisher) or CFSE, stimulated as mentioned above, and re-stained for cell surface markers.

Flow cytometry-based CTL cytotoxicity test

Assays to quantify the cytotoxic activity of CTLs were done by stimulating PBMCs with 30Gy irradiated autologous B-LCLs at 5:1 ratio in complete RPMI (Gibco)

with 10ng/mL IL-7 (Peprotech) for 14 days. At day 7, 100U/mL IL-2 (Peprotech) was added. Two rounds of stimulation were performed every 14th day. CD8^{+} T cells were sorted with MagniSort Human CD8^{+} T-cell Enrichment Kit according to manufacturer's instructions. Autologous EBV B-LCLs were stained with VPD450 (ThermoFisher) and used as targets. CD8+ T cells were incubated for 4 hours at different ratios of effector and target cells. Cytotoxicity was evaluated by flow cytometry gating on CD19^{+} and VPD450^{+} cells.

Flow cytometry-based CTL and NK-cell degranulation test

NK- and CTL degranulation was assessed by CD107a surface staining without (medium-cultured cells) and 3 hours after stimulation with K562 cells at a ratio of 1:1 as previously described[2]. The erythroleukemic cell line K562 (ATCC, CCL-243) was used as a target cell line. NK cells were cultured in medium containing 600U/ml IL-2 (Novartis) for 48 h to assess degranulation of activated NK cells. CTL (cytotoxic T lymphoblasts) degranulation was evaluated in T-lymphoblasts 48 h after stimulation with 1.25 mg/ml 1- phytohemagglutinin-L (PHA-L, Sigma) and 200U/ml IL-2 (Novartis). CTL degranulation was calculated by the difference in median fluorescence intensity of CD107a of CTLs stimulated with CD3/CD28-coated microbeads (ThermoFisher Scientific) at a ratio of 1:10 for 3 h and medium cultured
cells.

Flow cytometry and antibodies

For immunophenotyping the following antibodies were used: BV480 anti-CD45 (clone HI30, BD), APC-Fire 780 anti-CD3 (SK7, Biolegend), BUV395 anti-CD4 (RPAT4, BD), BUV496 anti-CD8 (RPAT8, BD), APC anti-CD45RA (BUV737, BD), BB515 anti-CD45RO (UCHL1, BD), APC anti-CD127 (A019D5, Biolegend), PE anti-CD25 (M-A251, BD), APC R-700 anti-CD27 (M-T271, BD), BB700 anti-CD28 (L293, BD), BV711 anti-HLA-DR (L243, Biolegend), BV421 anti-CCR7 (G043H7, Biolegend), BV786 anti-

CCR6 (11A9, BD), PE-CF594, anti-CXCR3 (1C6, BD), BV650 anti-CD38 (HB-7, Biolegend), BUV395 anti-CD19 (SJ25C1, BD), PE-Cy7 anti-CD20 (2H7, BD), BB515 anti-IgD (IA6-2, BD), BV421 anti-IgM (G20-127, BD), APC anti-CD38 (HB7, BD), BUV737 anti-CD21 (B-Ly4, BD), BV786 anti-CD27 (L128, BD), PE anti-CD10 (HI10a, BD), BUV496 anti-CD3 (UCHT-1, BD), BUV737 anti-CD8 (SK1, BD), PE-CF594 anti-CD56 (NCAM16.2, BD), BB515 anti-CD57 (NK-1, BD), BB700 anti-CD15 (M5E2, BD), APC anti-CD16 (3G8, Biolegend), HLA-DR anti-BV711 (L243, Biolegend), BV785 anti-CD123 (6H6, BD), BV421 anti-CD11c (B-ly6, Biolegend), PE anti TCR g-d (5A6.E9, Life Tech), APC-R700 anti-TCR a-b, (IP26, Biolegend), PE-Cy7 anti-CD33 (P67.6, BD), and BV711 anti-CXCR5 (J2252D4, Biolegend).

CD137 and CD137L expression in T cells was measured upon 48 hour stimulation of PBMCs with anti-CD3 and anti-CD28. Cells were stained with PacB anti-CD3 (clone SK7, biolegend), BV711 anti-CD4 (SK3, BD), APC-Fire 750 anti-CD8 (RPA-T8, Biolegend), PE anti-CD25 (M-A251, BD), APC anti-CD137 (4B4-1, BD) or APC anti-CD137L (5F4, Biolegend). Expression in B cells was measured upon 24 hour stimulation of PBMCs with anti-IgM in combination with CD40L (RnD). PBMCs were stained with PacB anti-CD3 (clone SK7, Biolegend), PerCP/Cy5.5 anti-CD19 (HIB19, Biolegend), BV421 anti-CD86 (FUN-1, BD), CD25 (M-A251, BD), APC anti-CD137 (4B4-1, BD). Expression in activated NK cells was measured upon 48 hours stimulation of PBMCs with IL-2 600U/ml (Novartis). PBMCs were stained with FITC anti-CD56 (NCAM16.2, BD), PacB anti-CD3 (SK7, Biolegend), APC anti-CD137 (4B4-1, BD).

Proliferative responses were measured by labeling PBMCs with 2.5 mM carboxyfluorescein diacetate succinimidyl ester (CFSE, ThermoFisher), 7-aminoactinomycin D (7-AAD, 2.5 mg/ml, BD), PacB-anti-CD3 (clone SK7, biolegend), PE-anti-CD25 (M-A251, BD), APC-Fire 750 anti-CD8 (RPA-T8, Biolegend)) and BV711 anti-CD4 (SK3, BD) 4 days after stimulation. Class-switch recombination and plamablast numbers were measured 4 days after stimulation. PBMCs were stained with BUV395 anti-CD3 (clone SK7, BD), PerCP/Cy5.5 anti-CD19 (HIB19, Biolegend),

BV421 anti-IgD (IA6-2, BD), PE anti-CD27 (L128, BD), BUV661 anti-CD38 (HIT2, BD). Degranulation of NK cells and CTLs (cytotoxic T lymphocytes) was determined by surface staining with PacB-anti-CD3 (clone SK7, 1:100), APC-H7-anti-CD8 (SK1, 1:100), PE-Dazz-anti-CD56 (NCAM16.2, BD), FITC anti-CD56 (NCAM16.2, BD), and PE-anti-CD107a (H4A3, 1:50). T-cell signaling was performed in T cell blasts. PBMCs were stimulated with 5 ng/ml phorbol 12-myristate 13-acetate (PMA) and 1 µM ionomycin (Sigma-Aldrich) and expanded with IL-2 (100U/ml) for 9 days. T-lymphoblasts were stimulated by cross-linking of anti-CD3 (UCHT1) 2.5 µg/ml and/or 10 µg/ml anti-CD28 (CD28.2) with 10 µg/ml goat anti-mouse IgG all from BD for the indicated time. Cells were fixed and permeabilized with fixation and permeabilization kit from Molecular Probes in 90% methanol. The permeabilized cells were stained with the following intracellular antibodies detecting: ERK1/2 phosphorylated at T202 and Y204 (A647 anti-pERK1/2, BD), NFκB P65 phosphorylated at S529 (A647 anti-NFκB P65, BD), AKT phosphorylated at S473 (A488 anti-pAKT, (M85-61, BD)), isotype control (A488 mouse IgG κ1 isotype control, BD).

TCR Repertoire and Analysis

Cell surface marker expression of peripheral blood mononuclear cells (PBMCs) was analyzed by immunofluorescent staining with monoclonal antibodies and flow cytometry (Epics V; Coulter Electronics, Hialeah, FL). Signal joint T-cell receptor excision circles (sjTREC) copy numbers were determined by employing quantitative real-time PCR (qRT-PCR) of genomic DNA (gDNA, 0.5 µg) extracted from whole blood of our patients. Surface expression of individual T cell receptor Vβ (TCR-Vβ) gene families was assessed using a set of 24 Vβ-specific fluorochrome-labeled monoclonal antibodies (Beckman Coulter, USA) and flow cytometry. Next-generation sequencing (NGS) T-cell receptor (TCR) libraries were generated from gDNA of patients and controls using primers for conserved regions of V and J genes in the *TRG* (T-cell receptor gamma) locus according to the manufacturer's protocol (Lymphotrack,

Invivoscribe Technologies, Carlsbad, CA). Quantified libraries were pooled and sequenced using Mi-Seq Illumina technology (Illumina, USA). FASTA files from the filtered sequences were submitted to the IMGT HighV-QUEST webserver (http://www.imgt.org), filtered for productive sequences (no stop codons or frameshifts), and analyzed Repertoire diversity was calculated using Shannon's H diversity index and Simpson's D index of uneveness.

Shannon's H index: $H' = -\sum_{i=1}^{R} p_i \ln p_i$

Simpson's D index of unevenness: $\lambda = \sum_{i=1} p_i^2$

Retroviral Construction and Transfection Protocol

N-terminally tagged CD137 was generated using retroviral pfMIG 3981 (IRES-GFP) vector. For the reconstitution experiments constructs with either wild-type CD137 or empty vector (GFP only) were used. Before electroporation of the Patient 3 and healthy donor PBMCs, retroviral vector was digested with Xba I enzyme to generate 3 kb DNA fragment containing CD137-IRES-GFP gene sequences. Digested DNA was purified using QIAquick PCR purification kit (Qiagen) according to manufacturer instructions. Patient 3 and healthy donor PBMCs were electroporated with 2µg of the digested DNA mixture using Amaxa Human T cell Nucleofector Kit (Lonza), program V-024, according to manufacturer instructions. Transfection efficiency was assessed by GFP expression 24 hours after electroporation.

Statistical Analysis

Statistical evaluation of experimental data was performed using Prism version 6 (GraphPad Software, USA). Probability (*P*) values < 0.05 were considered statistically

significant. *P* values and statistical tests are indicated in figure legends, where applicable.

Supplementary References

1. Adzhubei I, Jordan DM, Sunyaev SR. Predicting Functional Effect of Human Missense Mutations Using PolyPhen-2. Current protocols in human genetics / editorial board, Jonathan L Haines [et al]. 2013 Jan;0 7:Unit7 20.

2. Bryceson YT, Pende D, Maul-Pavicic A, Gilmour KC, Ufheil H, Vraetz T, et al. A prospective evaluation of degranulation assays in the rapid diagnosis of familial hemophagocytic syndromes. Blood. 2012 Mar 22;119(12):2754-63.

Table S1. Clinical and genetic manifestations of CD137-deficient patients

Patients	P1	P2	P3	P4	*Pa	*Pb
Mutation	c.1_545+1716del	NM_001561.5: c.452C>T; p.Thr151Met	NM_001561.5: c.101 -1G>A	NM_001561.5: c.100 +1G>A	NM_001561.5: c.325G>A p.Gly109Ser	NM_001561.5: c.325G>A p.Gly109Ser
Initial clinical manifestation	abdominal distention	recurrent respiratory infections	lower respiratory tract infection	recurrent infections from childhood	sinopulmonary infections, bronchiectasis, pneumococcal septicemia	recurrent sinopulmonary infections, generalized lymphadenopathy, EBV viremia
Age of initial Clinical manifestation	2 years	4 years	6 years	8 years	3 years	6 years
Consanguinity	parents are 1st degree cousins	parents are 1st degree cousins	parents are 3rd degree cousins	no known consanguinity	parents are 1st degree cousins	parents are 1st degree cousins
Infectious complications during disease course	recurrent ear infections EBV viremia	recurrent pneumonia EBV viremia	recurrent labial herpes, recurrent tonsillitis, recurrent otitis media, recurrent pneumonia EBV viremia	recurrent ear infections, recurrent pneumonia, pleuropneumonia, chronic sinusitis EBV viremia	pneumococcal septicemia sinopulmonary infections EBV viremia	sinopulmonary infections EBV viremia
Identified Pathogens	CMV, EBV	*adenovirus,* EBV, HSV	EBV, HSV	EBV	*streptococcus pneumoniae,* EBV	EBV
Hepatosplenomegaly	+	+	+	+	splenomegaly	splenomegaly
Lymphadenopathy	-	+	+	-	+	+
Malignancy	CD20 positive Burkitt lymphoma	-	EBV-positive Hodgkin's lymphoma	-	-	EBV-positive Hodgkin´s lymphoma, relapse and progression to DLBCL

Treatment of B-cell malignancies	cytoreductive prophase treatment: cyclophosphamide, dexamethasone, methotrexate (AA, BB, CC blocks), rituximab	NA	etoposide, doxorubicin, vincristine	NA	NA	5 cycles: doxorubicin, bleomycin, vincristine, etoposide, prednisone, cyclophosphamide along with rituximab; upon relapse daratumumab, bortezomib, dexamethasone and rituximab
AIHA	-	+	+	-	-	-
ITP	-	+	-	-	-	-
Other features	-	ALPS like symptoms, EBV associated lymphoproliferation	short stature	distal peptic esophagitis, erythematous gastritis	hemophagocytic lymphohystiocytosis	-
Treatment of immunodeficiency/Infections	IVIG, co-trimoxazole, fluconazole	sirolimus, cellcept, co-trimoxazole	IVIG, antibiotic prophylaxis	SCIg	IVIG, rituximab	IVIG
Outcome	responded well to chemotherapy treatment protocol and rituximab, currently stable under IVIG and antibiotic prophylaxis	well on cellcept treatment and co-trimoxazole antibiotic prophylaxis	good response to chemotherapy with clinical remission. Currently stable under IVIG and antibiotic prophylaxis	stable under SCIg replacement treatment with resolution of infections	sinopulmonary infections improved upon IVIg treatment, resolution of viremia with rituximab. Currently undergoing HSCT from a healthy HLA-matched sibling	clinical remission and resolution of viremia with chemotherapy and rituximab treatment. Respiratory tract infections improved with IVIg treatment

CMV: Cytomegalovirus. EBV: Epstein-Barr virus. HSV: Herpes simplex virus. NA: Not applicable. AIHA: Autoimmune hemolytic anemia. ITP: Immune thrombocytopenic purpura.

ALPS: Autoimmune lymphoproliferative syndrome. IVIG: Intravenous immunoglobulin. SCIg: Subcutaneous immunoglobulin. HSCT: hematopoietic stem cell transplantation.

DLBCL: diffuse large B cell lymphoma.

*Pa, Pb reported by Alosaimi et al. *J Allergy Clin Immunol*, 2019.

Table S2. Immunologic characteristics of patients with CD137 deficiency

Variable	Patient 1		Patient 2		Patient 3		Patient 4	
	Value	Reference Range	Value	Reference Range	Value	Reference Range	Value	Reference Range
Age of evaluation	4 years		9 years		11 years		33 years	
Absolute lymphocyte count (cells/mm^3)	3390	2340-5028	3597	1300-5000	1590	1300-3000	2680	1200-4100
Lymphocyte subset								
CD3+ (cells/mm^3)	1551	1239-2611	2950	700-4200	1272	1000-2000	1860	780-3000
CD4+ (cells/mm^3)	1074	870-2144	1295	600-2100	858	500-1300	965	100-2300
CD45RO+ CCR7+ (%)	**7.5**	13.88-48.12	**14.6**	22.06-46.46	45.5	24.24-52.73	**11.5**	18-95
CD45RO+ CCR7- (%)	**78.7**	0.94-6.46	**59.3**	2.08-8.78	**26.5**	3.4-11.17	**55.8**	1-23
CD45RO- CCR7+ (%)	**11.6**	46.14-84.4	**22**	45.56-75.28	**24.5**	39.72-69.59	**27**	16-100
CD45RO- CCR7- (%)	1.1	0-1.36	0.1	0-1.06	**2.43**	0.1-1.29	5.7	0-6.8
CD8+ (cells/mm^3)	**407**	472-1107	**1439**	200-1100	333	300-800	772	200-1200
CD45RO+ CCR7+ (%)	**0.9**	5.18-31.66	**3.4**	12.08-30.54	**4.9**	13.21-37.89	7.3	1-20
CD45RO+ CCR7- (%)	**62.4**	0.7-11.22	**43.3**	1.58-13.18	15.2	1.53-15.39	29.3	14-98
CD45RO- CCR7+ (%)	**3.8**	36.8-83.16	**34.8**	41.58-77.9	**77.1**	41.41-73.04	23.7	41.41-73.04
CD45RO- CCR7- (%)	29.7	0.84-33.02	15.3	1.7-24.62	2.79	2.01-21.65	36.2	2.01-21.65
CD3-CD16+CD56+ (cells/mm^3)	176	155-565	**54**	120-483	**76**	100-700	417	90-600
CD19+ (cells/mm^3)	846	434-1274	**360**	50-300	238	200-500	278	100-500
IgD+ CD27- (%)	**93**	73-89	**94.6**	67.8-89	**93.7**	67.8-89	**95.5**	58-72.1
IgD+ CD27+ (%)	**2.2**	5.7-14.3	**2.1**	5-16.2	**1.83**	5-16.2	**1.9**	13.4-21.4
IgD- CD27+ (%)	**1.2**	3-10.3	**0.9**	4-14	**0.79**	4-14	**1.8**	9.2-18.9
CD27+ CD38+ (%)	0.76	0.5-7.06	**0.70**	0.9-7.36	**0.37**	0.7-5.67	**0.61**	0.9-7.36

Immunoglobulins								
IgG (mg/dL)	**413**	701-1157	**1599**	540-1550	**2290**	824-1300	**550**	968-2514
IgM (mg/dL)	105	42-80	**714**	40-240	**267**	44-142	**33.6**	103-397
IgA (mg/dL)	68.7	34-108	**49**	52-274	130	71-161	**31**	103-397
IgE (IU/mL)	26.4	2-199	0	0-200	7.77	<100	173	116-551
Complement								
C3(mg/dL)	N/A		**68.9**	90-180	105	90-180	N/A	
C4(mg/dL)	N/A		**72.4**	10-40	**9.3**	10-40	N/A	
T-cell repertoire								
αβ+ (%)	94		79		83		95.3	
γδ+ (%)	**2**	4.94-17.98	**2**	6.92-19.84	**1.1**	8.1-20.76	3.5	
TRECs	N/A		800	>400	N/A		N/A	
Auto-immune workup								
Positive auto-antibodies			ANA positive (1:180)		d. Coombs positive			
EBV/CMV status								
EBV DNA Viral Load (PCR)	**652 copies/ml**		**7.1 X10^5 copies/ml**		**9.1 X10^4 IU/ml**		**610 Geq/ml**	
CMV DNA Viral Load (PCR)	**82 copies/ml**		negative		NA		negative	
EBV Serology	NA		EBNA-1 (IgG): positive		*EBNA-1 (IgG): positive *VCA (IgM): negative *VCA (IgG): positive		NA	

CMV Serology	NA	anti-CMV (IgG): negative	*anti-CMV (IgM): **2.44** (>1.1 U/ml) *anti-CMV (IgG): positive avidity = 0.837 positive	NA
Common vaccine serologies				
Rubella Serology	&anti-rubella (IgG): 101.3 IU/ml (positive)	MMRV serology (IgG): positive	anti-rubella (IgG): 59.3 IU/ml (positive)	*anti-rubella (IgG): **0.94 uL/mL (negative)** Sister: anti-rubella (IgG): 15.2 uL/mL (positive)
Varicella Serology	&anti-VZV (IgG): 1141 IU/ml (positive)		NA	NA
Hepatitis Serology	&anti-HBs (IgG): 201.4 uL/ml (positive)	anti-HAV (IgG): positive anti-HBs (IgG): **negative**	NA	NA
Tetanus Serology	&anti-tetanus (IgG): 2.8 U/ml (positive)	NA	anti-tetanus (IgG): 2.8 U/ml (positive)	NA

Listed are reference ranges or laboratory values for the patient's age group. Abnormal values in **bold**.

CMV Cytomegalovirus; EBNA Epstein Barr Nuclear Antigen; EBV Epstein Barr Virus; HAV Hepatitis A virus; HBV Hepatitis B virus; MMRV Measles, Mumps, Rubella, Varicella; NA Not Applicable; VCA Viral-Capsid Antigen; VZV Varicella Zoster Virus.

*Prior to IVIg / SCIg replacement therapy; &On IVIg replacement therapy

Table S3. Summary of homozygous autosomal recessive mutations in patients

Patient	Gene	Chromosome	Position	Reference	Variant in patient	Mutation type	Protein variant in patient
1	*ZXDB*	X	57620724	T	A	MISSENSE	p.Val748Asp
1	*TNFRSF9*	1	7995072-8000054	NA	NA	DELETION	NA
1	*PARK7*	1	8022845-8031023	NA	NA	DELETION	NA
2	*XIST*	X	73048904	A	G	SPLICE REGION	NA
2	*AFF2*	X	148048444	C	T	MISSENSE	p.Thr1013Met
2	*TNFRSF9*	1	7995165	C	T	MISSENSE	p.Thr151Met
2	*METTL18*	1	169763046	C	A	SPLICE REGION	NA
2	*GPC1*	2	241375361	GGCT	G	DELETION	p.Leu11del
2	*DNAH5*	5	13794053	G	A	MISSENSE	p.Gly2668Arg
2	*CD36*	7	80293747	A	G	MISSENSE	p.Tyr212Cys
3	*ASB12*	X	63445095	C	G	MISSENSE	p.Ala146Pro
3	*TNFRSF9*	1	7998889	C	T	SPLICE SITE ACCEPTOR	NA
3	*HS6ST1*	2	129075797	A	C	MISSENSE	p.Val114Gly
3	*IRX4*	5	1880839	C	T	MISSENSE	p.Arg136Lys
3	*ZNF808*	19	53058034	C	T	MISSENSE	p.Pro622Leu
4	*TNFRSF9*	1	799954	G	A	SPLICE SITE DONOR	NA

Inclusion criteria:
CADD more than 15
SIFT deleterious
Polyphen probably_damaging

Table S4. Predicted impact scores of *CD137* variants

Patient	Mutation	Chromosome	Position	PolyPhenCat	SIFTcat	CADD
1	c.1_545+1716del	1	7995072-8000054	NA	NA	NA
2	c.452C>T	1	7995165	Probably_damaging	Deleterious	24.9
3	c.101 -1G>A	1	7998889	NA	NA	27
4	c.100 +1G>A	1	799954	NA	NA	25

Supplementary Figures legends

Figure S1. Clinical features, radiology, pathology, T cell clonality. (A) Coronal T2-HASTE image (Patient 1) demonstrating multiple hypointense metastatic renal cortical masses (black arrows). A mass lesion is observed on the right paraspinal area infiltrating the adjacent paravertebral muscle (red arrow). (B) Chest CT scan demonstrating consolidation in the anterior aspect of the right middle lobe (RML), nodular opacity in the lingula and posterior mediastinal adenopathy (Patient 2). (C) Coronal reconstructions of a follow-up CT four months later demonstrating ground glass opacities in both lungs (Patient 2). (D) Splenomegaly (Patient 2) shown in coronal reconstruction of CT scan. (E) CT scan of the upper neck showing cervical lymphadenopthy (Patient 2). (F) Contrast enhanced computerized tomography (CT) demonstrating mediastinal and axillary lymphadenopathy (Patient 2). (G) Coronal reconstruction of Positron Emission Tomography showing increased uptake in the cervical, axillary and mediastinal lymph nodes. An infiltrate in the right middle lobe (RML) is demonstrated. (H) TCR-gamma spectratyping of lymph node biopsy (Patient 2) revealing two dominant peaks, supporting the presence of a monoclonal T-cell population. (I) In situ hybridization for EBV-encoded small RNAs (EBER) displaying numerous positive cells (Patient 2). Sections used are from right inguinal lymph node tissue. (J) Abdominal CT scan (Patient 3) demonstrating hepatomegaly. (K) MR demonstrating chronic sinusitis in Patient 4 with obstruction in Lt. sinus.

Figure S2. Genetic analysis. Sanger sequencing chromatograms confirming the WES findings in Family B, Family C and Family D. For Family A, WES reads in Patient 1 are compared to a healthy control showing no NGS coverage for several exons of *TNFRSF9* and *PARK7*.

Figure S3. *TNFRSF9* sequence homology in species. *TNFRSF9* sequence alignment showing the conservation of amino acid threonine at position 151 across eight species (red frame). The variant in Patient 2 (p.Thr151Met) is stated.

Figure S4. Effect of variants in the patients. (A) (upper left) Amplified gDNA utilizing forward and reverse primers to amplify exon 6 in *TNFRSF9* for Family A and controls, depicting the genomic deletion in patient 1 (AII-1) and brother (AII-2). Full length cDNA of Patient 3 (CII-2) (upper middle panel) and Patient 4 and sister (DII-1) (upper right panel) were amplified and loaded on agarose gels, depicting smaller sized bands. * and ** in middle panel depicts two aberrantly spliced transcripts. (B) Schematic illustration showing the consequences for the splice site variants in Patient 3 and Patient 4. cDNA sequencing results revealed a skipping of exon 2 in Patient 4, and a skipping of exons 3 and 6 for Patient 3. (C) Chromatograms of Sanger sequencing of the PCR product marked * and ** in figure A showing skipping of exon 3 and exons 3 and 6 in P3.

Figure S5. CD137 expressions. Flow-cytometric expression of CD137 in unstimulated and anti-CD3/CD28 stimulated T-cells for patients, siblings and heathy donors (HDs) are shown.

Figure S6. (A) Peripheral blood B-cell immunophenotyping: Memory ($CD19^+CD20^+CD27^+$), class-switched ($CD19^+CD20^+CD27^+IgD^-$) and transitional B-cell ($CD19^+CD38^+IgM^+$) frequencies are compared in patients and siblings, measured by flow-cytometry. (B) Peripheral blood T-cell immunophenotyping: Follicular helper T-cell (T_{FH}) frequencies are shown in patients and siblings, measured by flow-cytometry.

Figure S7. CD137 and CD137L inhibition in T-cell function. (A) Effect of CD137 blockade on proliferation of T-cells in healthy donors (HDs). Anti-CD137 monoclonal neutralizing antibody (BBK-2 clone) or isotype control was added to anti-CD3 stimulation at increasing concentrations showing a dose dependent inhibition of T-cell proliferation (as

measured by VPD450 dilution). Error bars indicate ± SEM. (B) T-cell activation (CD25 expression): Flow-cytometric expression of $CD25^+$ is depicted in patients and HDs upon 96 hour stimulation with anti-CD3, anti-CD3+CD137L and anti-CD3+CD28. (C) Restoration of T-cell activation upon CD137 expression. CD137 expression, CD25 T-cell activation and rate of proliferated T cells (stimulated with anti-CD3) upon exogenous expression of wild-type CD137 are shown in Patient 3. (D) *TNFSF9* mRNA expression (top panel) and CD137L surface expression (bottom panel) was measured in unstimulated and anti-CD3+anti-CD28 stimulated T-cells. *HPRT* was used as a control.

Figure S8. Cytotoxicity, degranulation and T cell receptor mediated signaling. (A) EBV-specific CTL cytotoxicity measured by the percentage of specific lysis of autologous EBV B-LCL target cells by their respective $CD8^+$ T-cells at different effector to target ratios. Patient CTL cytotoxicity showed significant reduction compared to HDs (* *P* value<0.05, Two-way ANOVA). (B) CTL degranulation (CD107a) was measured in stimulated $CD8^+$ T-cells by flow cytometry. (C) NK-cell degranulation in patients and HDs is compared in unstimulated and stimulated PBMCs, measured by flow-cytometry. (D) Immunoblotting showing expression of IκBα, phospho-p65, total p65, phospho-AKT and total AKT upon anti-CD3+CD28 stimulation in expanded T cells. HSP90 was used as a loading control. Intracellular phospho-AKT and NF-κB1 phospho-p65 levels in unstimulated and stimulated T-cell blasts, measured by flow cytometry. (E) MAPK signaling is shown measured by immunoblotting. Immunoblotting expression of total ERK1/2 and phospho-ERK1/2 upon anti-CD3+CD28 stimulation in expanded T-cells. HSP90 was used as a loading control. Intracellular phospho-ERK levels in unstimulated and stimulated peripheral $CD4^+$ and $CD8^+$ T-cells is depicted, measured by flow cytometry.

Figure S9. *In vitro* plasmablast differentiation. (A) Plasmablast ($CD3^-CD19^+CD27^+CD38^+$) frequencies are shown in unstimulated PBMCs and upon 96 hour stimulation with CpG,

CD40L+IL4 and CD40L+IL21, showing a significant difference between HDs and Patients. (* *P* value<0.05, ** *P* value<0.01, **** *P* value<0.0001, Two-way ANOVA). (B) CD137L expression in $CD19^+$ B-cells upon CpG stimulation measured by flow cytometry, showing expression of CD137L in both HD and Patient 3 stimulated cells.

Figure S10. Naïve B-cell function. Naïve B-cells ($CD19^+CD3^-IgD^+CD27^-$) were sorted and B-cell functions were assessed in our patients. (A) $CD86^+$ B-cell activation was measured 1 day post-stimulation with CpG, showing reduced B-cell activation in P3 and P4. (B) naïve B-cell proliferation measured by violet proliferation dye (VPD450) 5 days post-stimulation showing reduced rate of proliferating B-cells in P3 and P4 in response to T-cell dependent (CD40L + IL21) and independent (CpG) stimuli. (C) Class switch recombination in sorted naïve B-cells. Gating of class switched IgG^+ and IgA^+ of sorted naïve B-cells upon CD40L + IL21 and CpG stimuli, depicted reduced CSR in P3 and P4. (D) Reduced memory B cells rates in P2 and P4 upon CpG stimulation of sorted naïve B-cells.

Supplementary Figure 1

Clinical Features, radiology, pathology，T-cell clonality

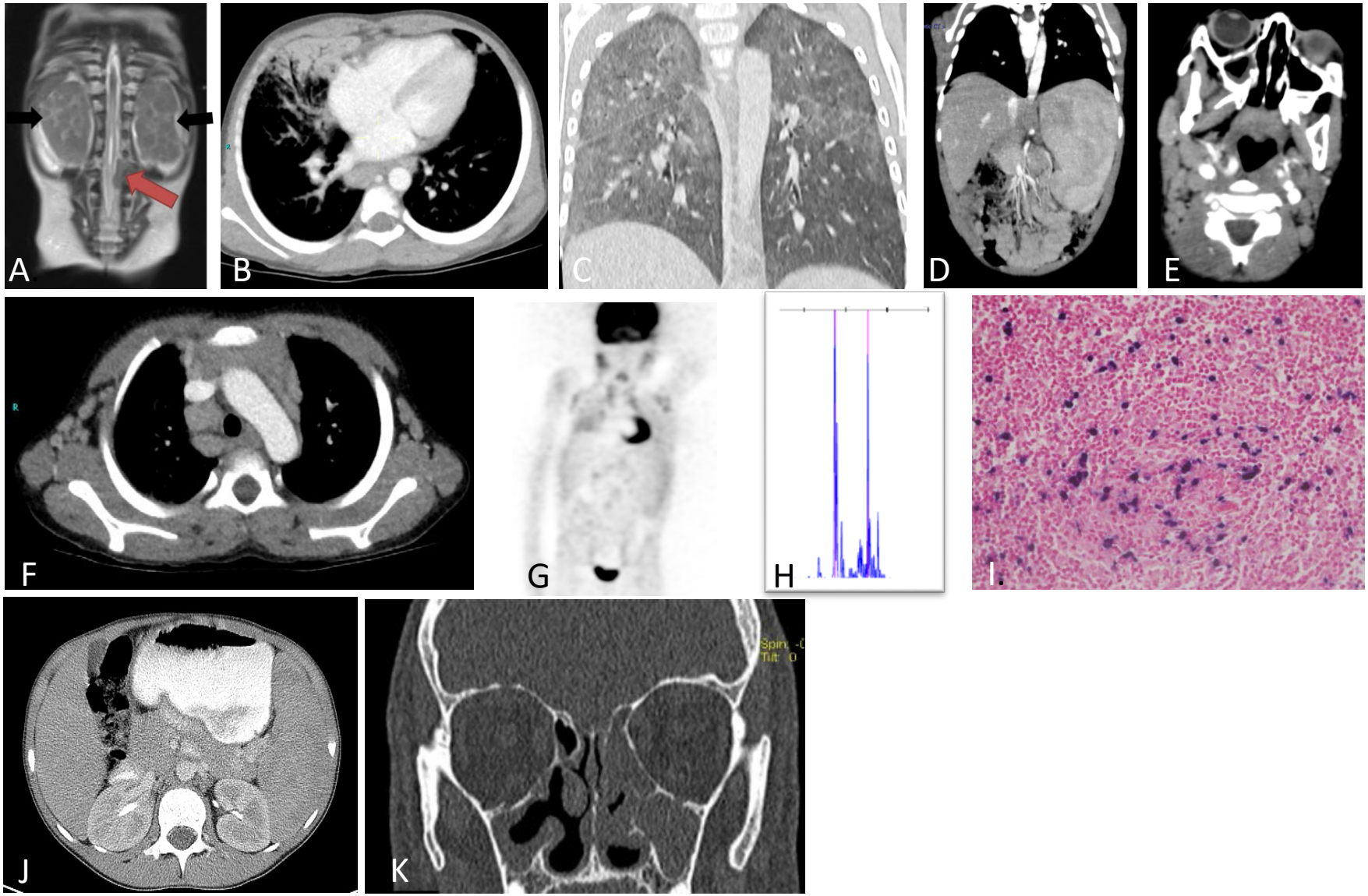

Supplementary Figure 2

Genetic analysis

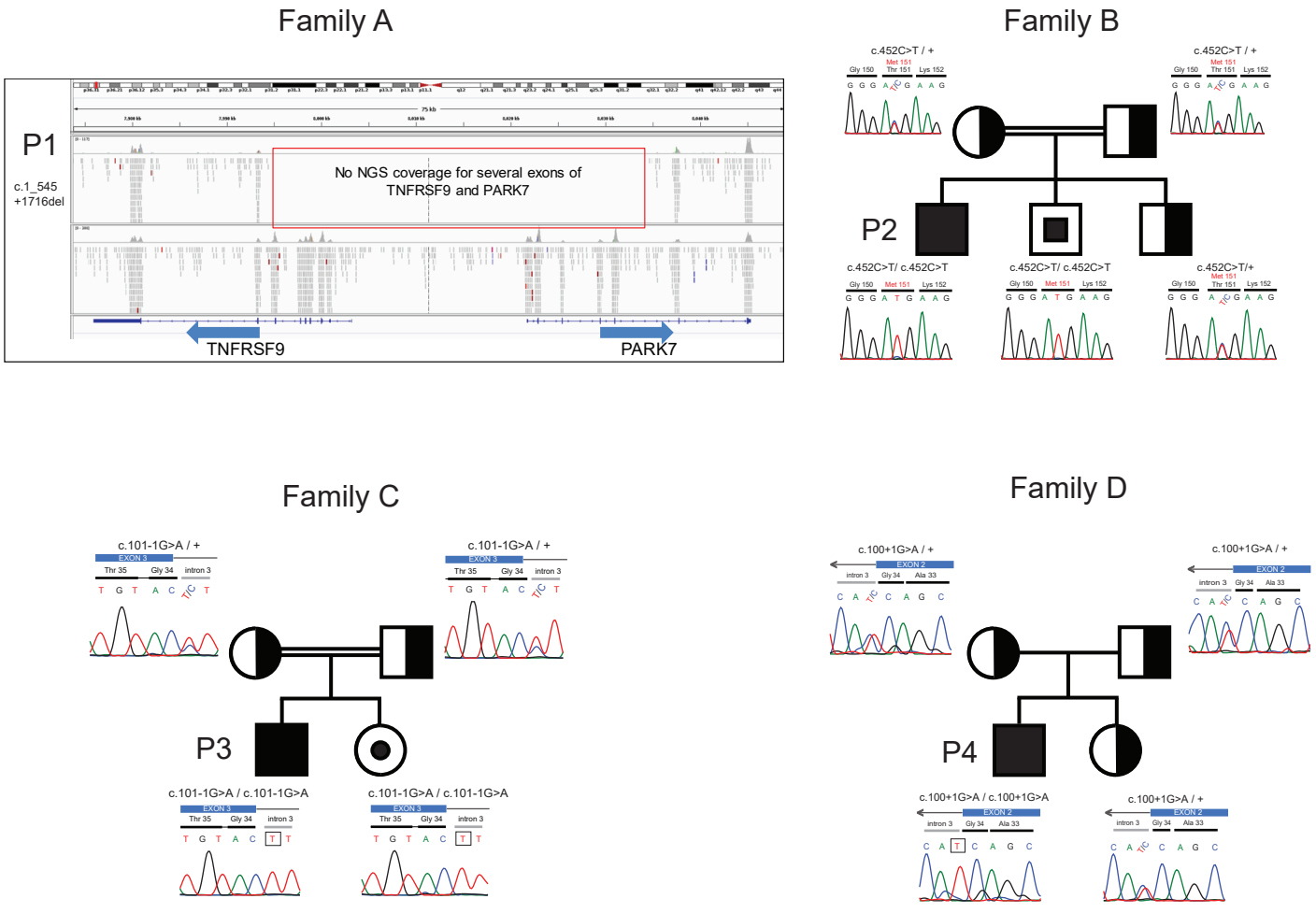

Supplementary Figure 3

TNFRSF9 sequence homology in species

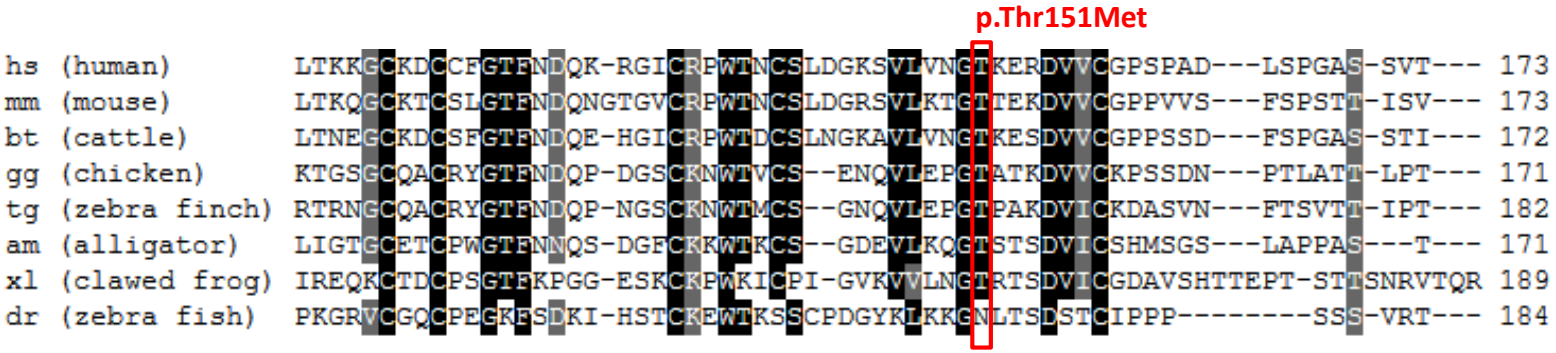

Supplementary Figure 4

Effects of variants in the patients

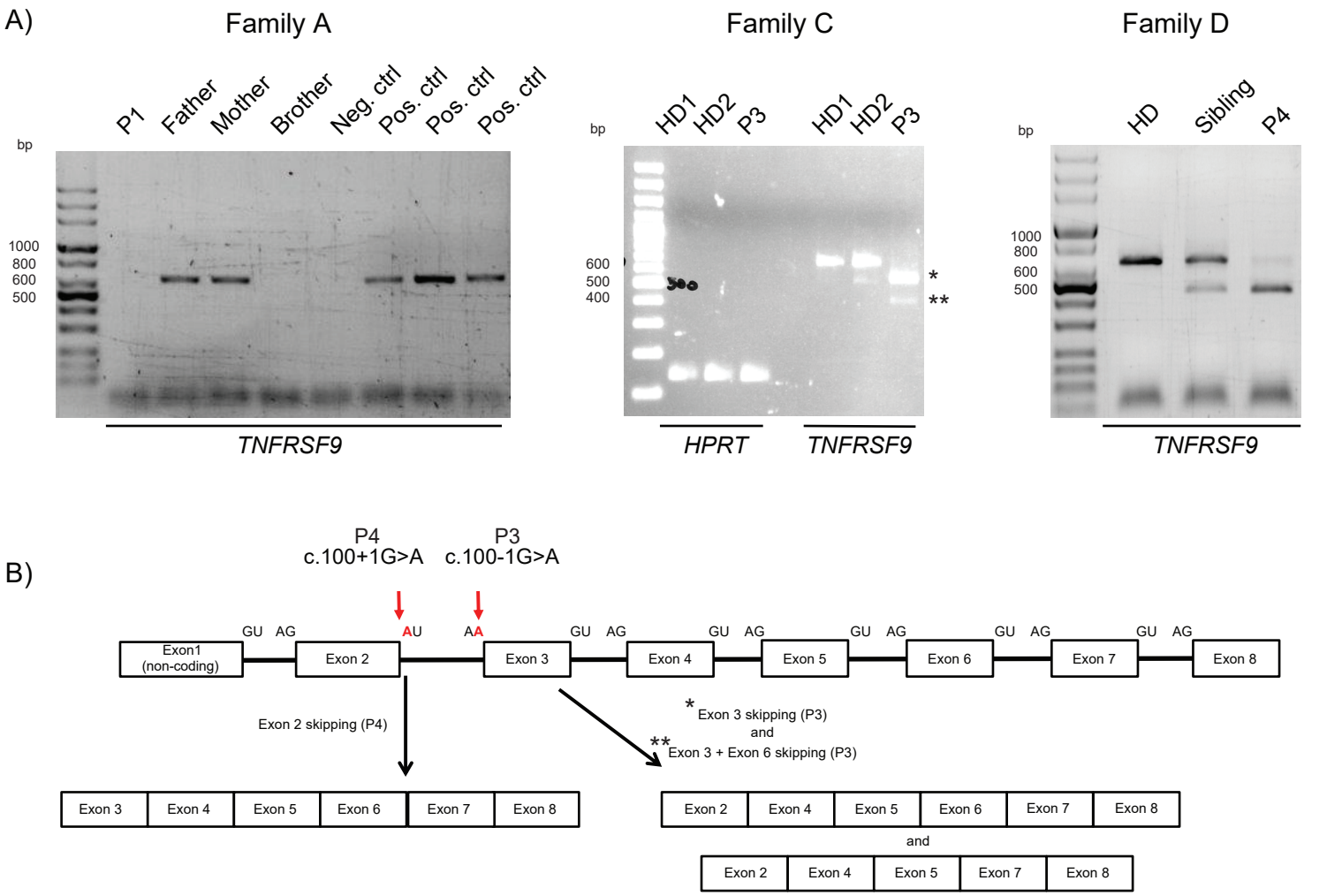

Supplementary Figure 5

CD137 expression

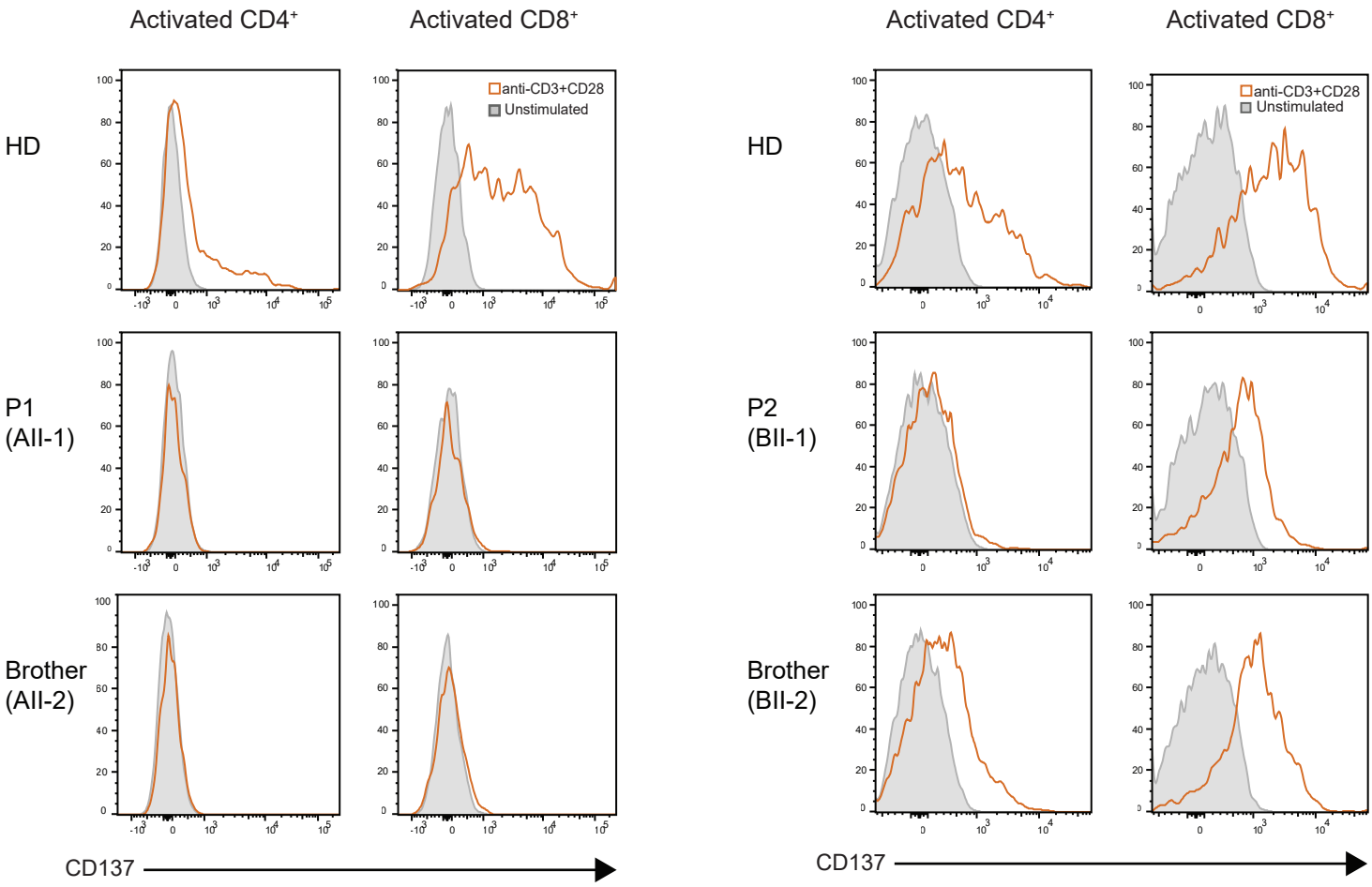

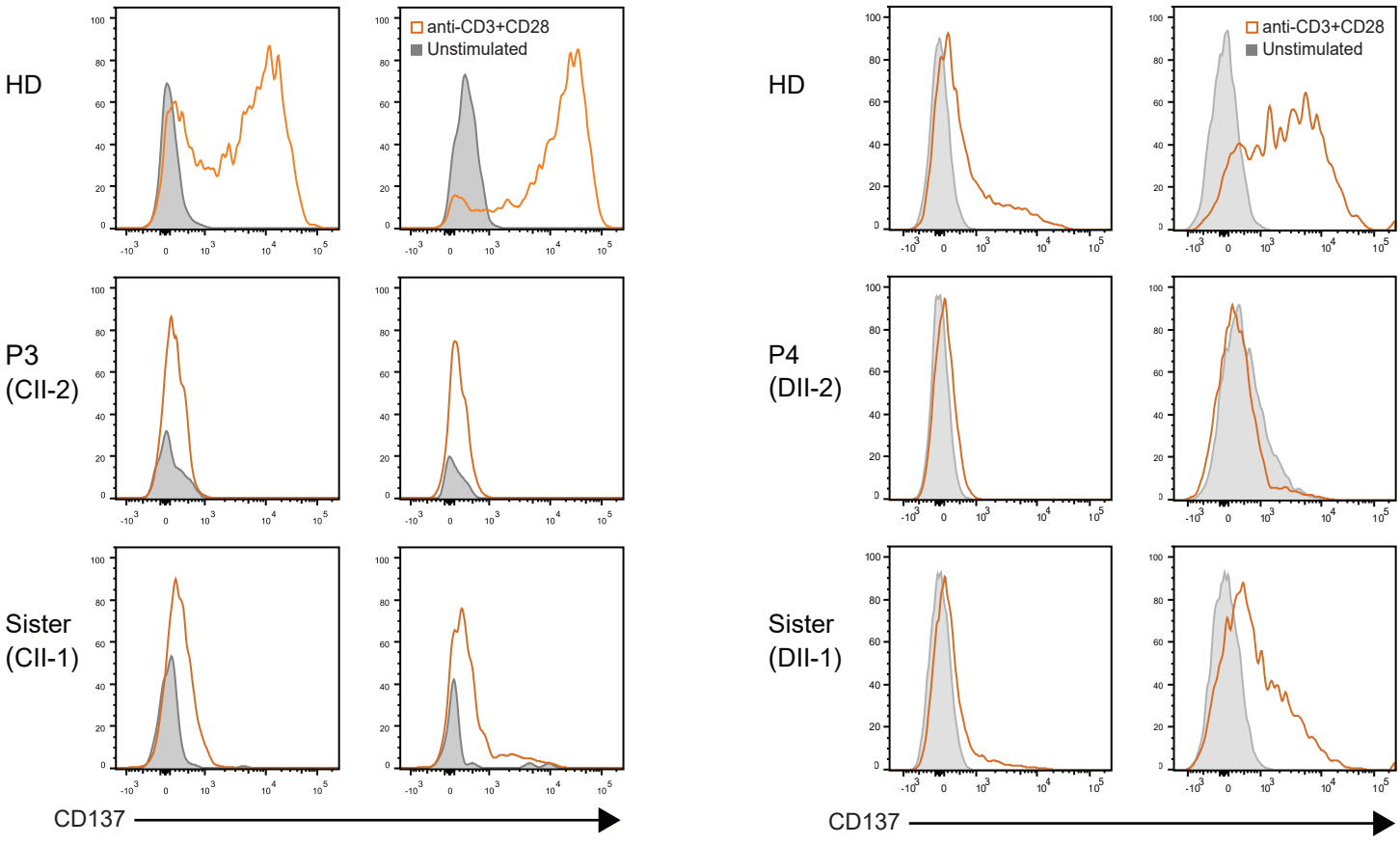

Supplementary Figure 6a

Peripheral blood B-cell immunophenotyping

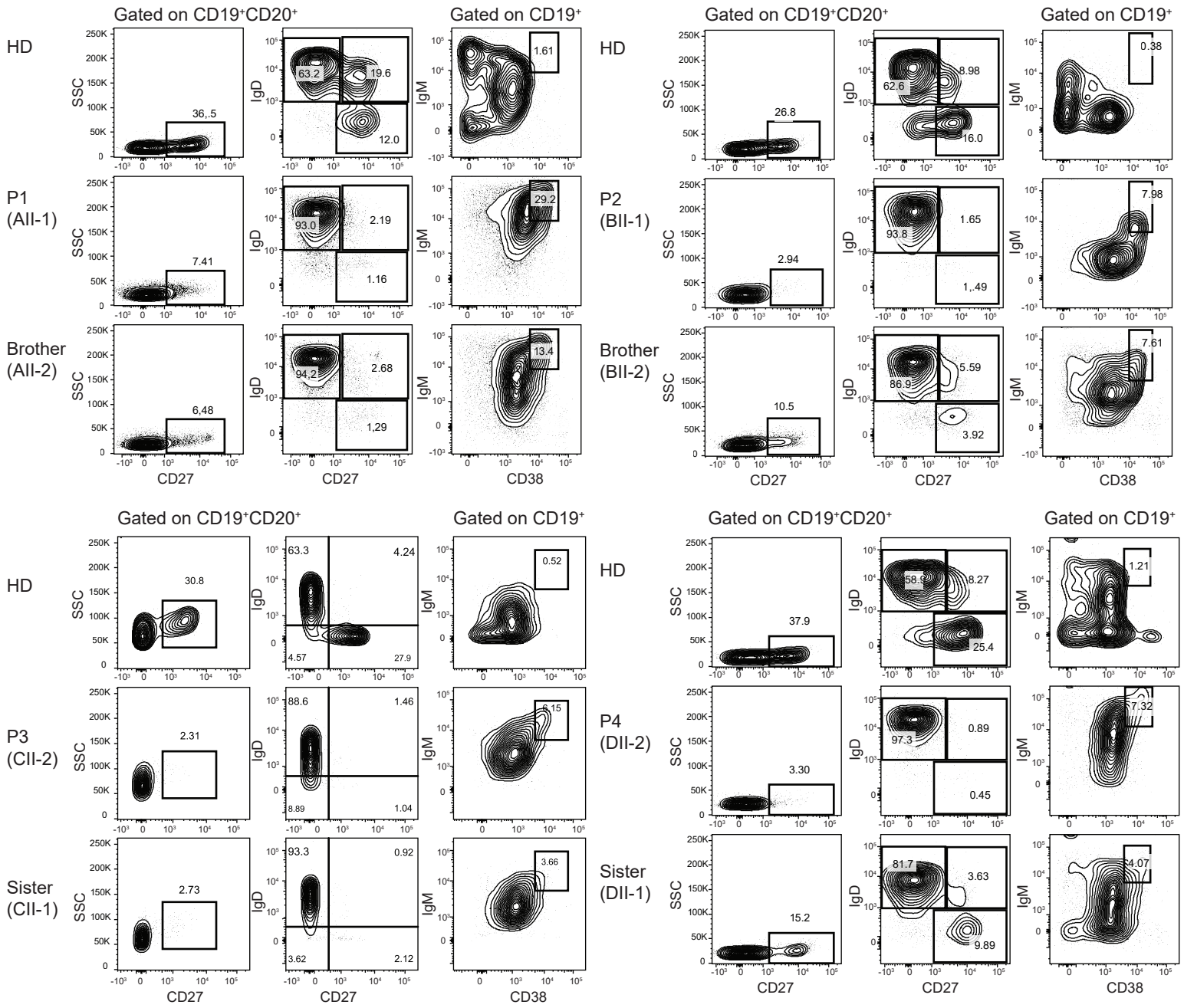

Supplementary Figure 6b

Peripheral blood T-cell immunophenotyping

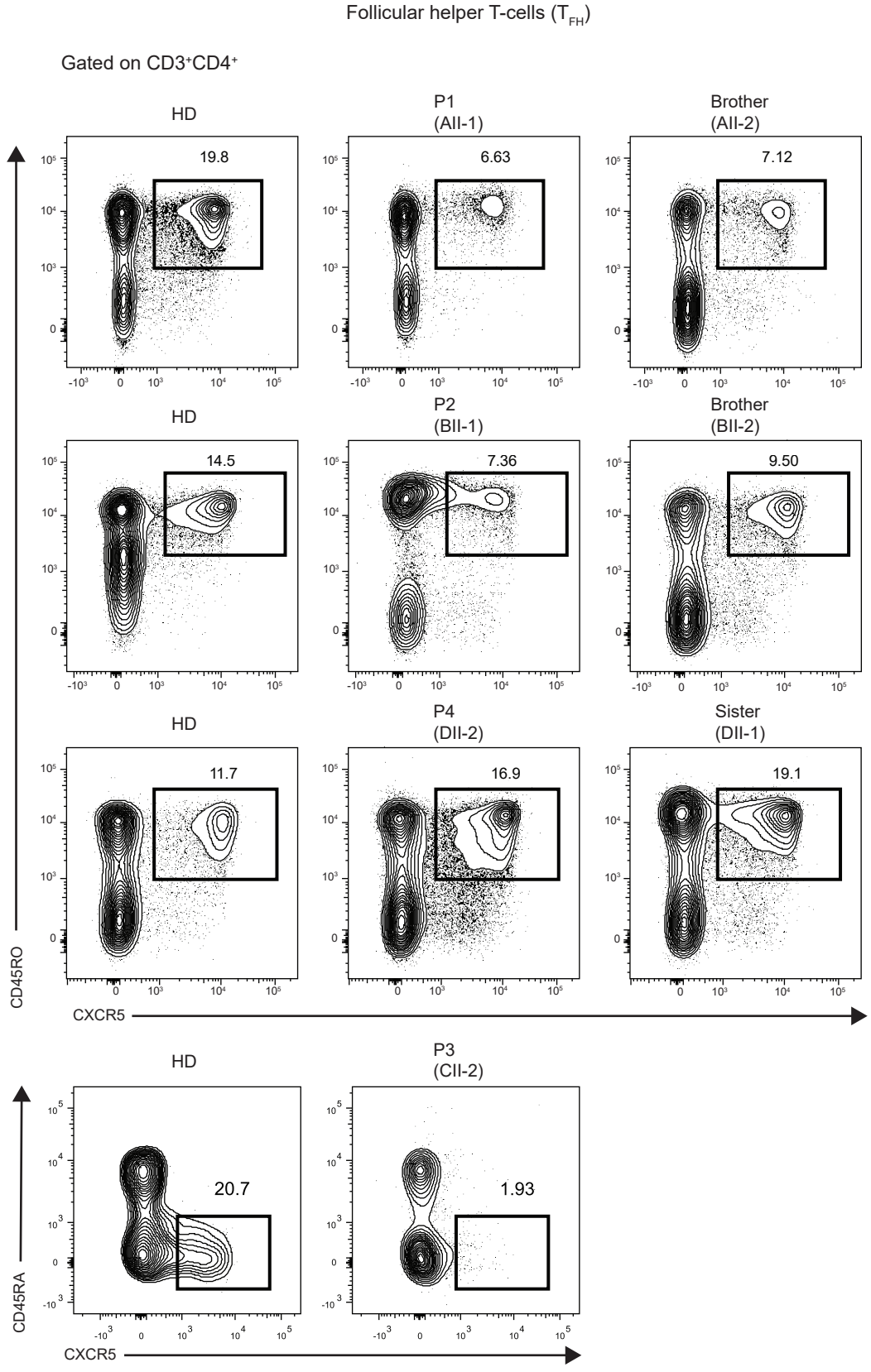

Supplementary Figure 7

A Blocking CD137 in HD T-cells

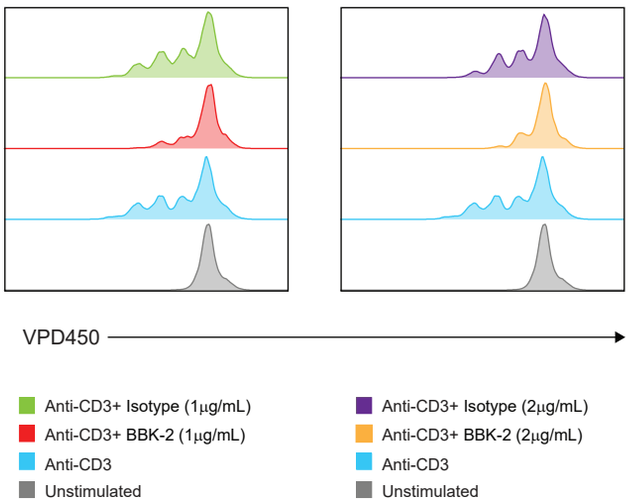

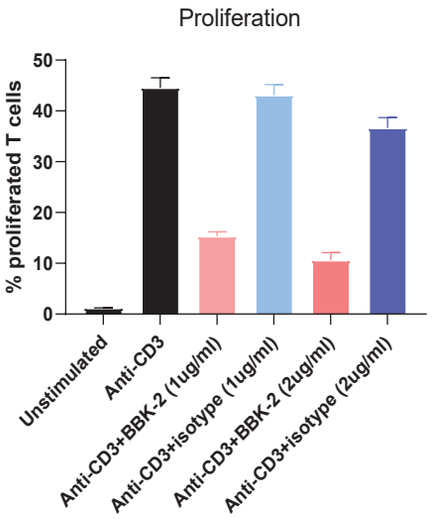

B T-cell activation (CD25 expression)

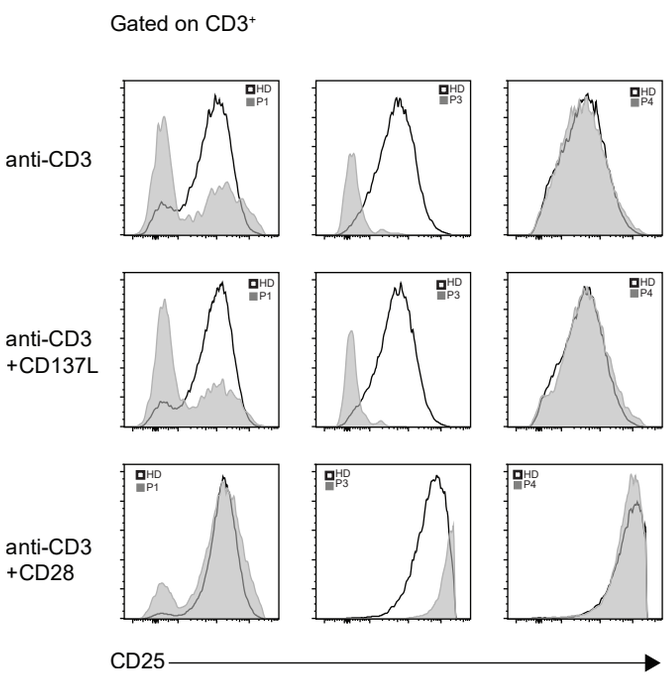

C Reconstitution of CD137 upon stimulation with anti-CD3 alone

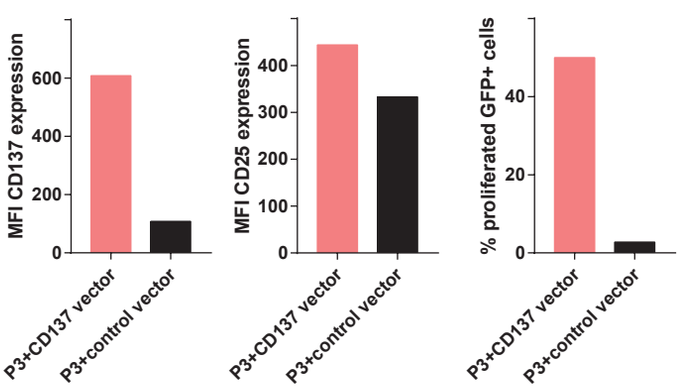

D *TNFSF9* and CD137L expression in T-cells

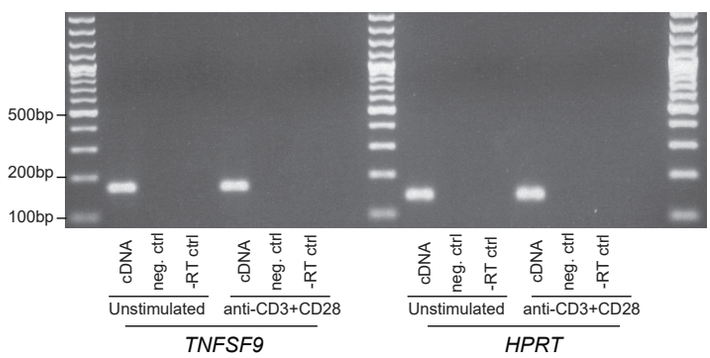

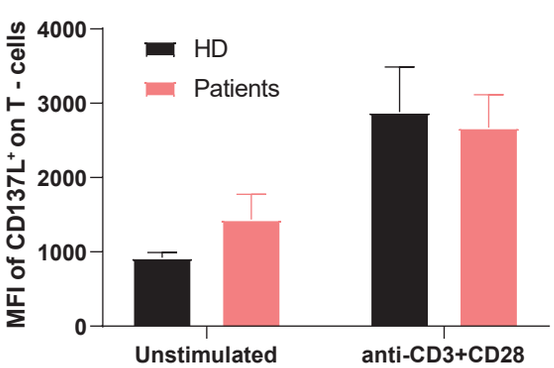

Supplementary Figure 8

CTL cytotoxicity, NK-cell degranulation and T-cell receptor mediated signaling

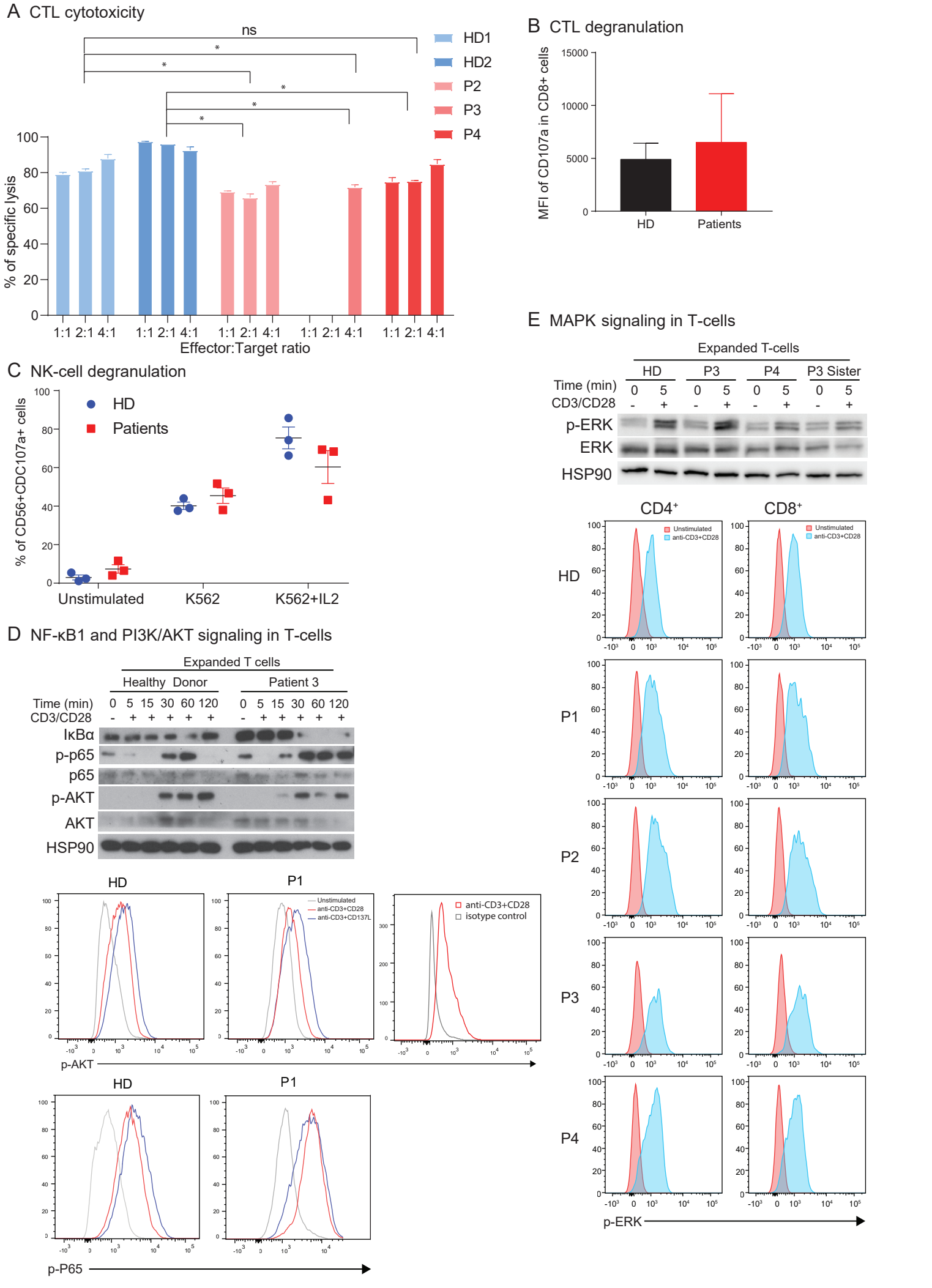

Supplementary Figure 9

A *In vitro* plasmablast differentiation

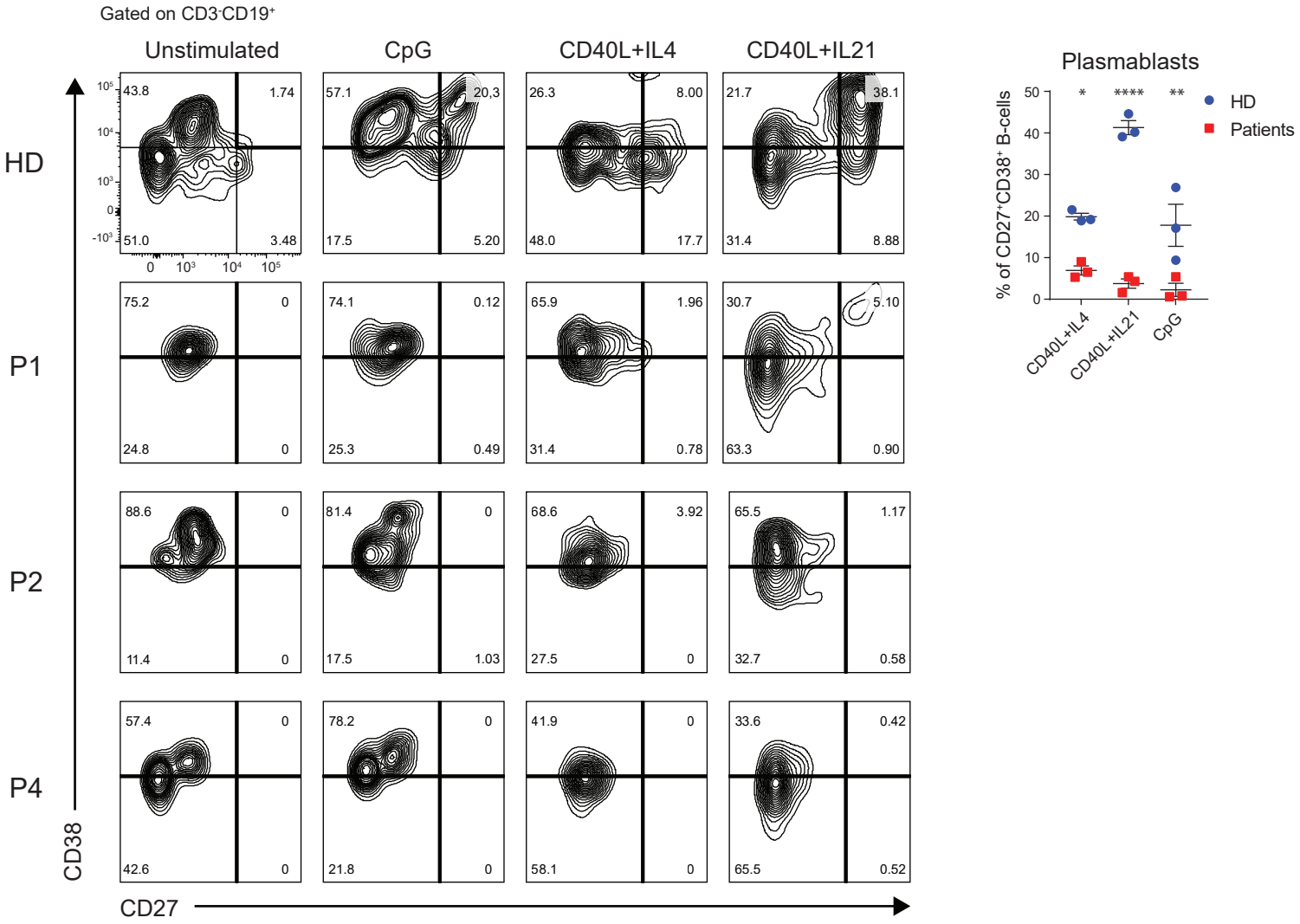

B CD137L expression on CD19⁺ B-cells

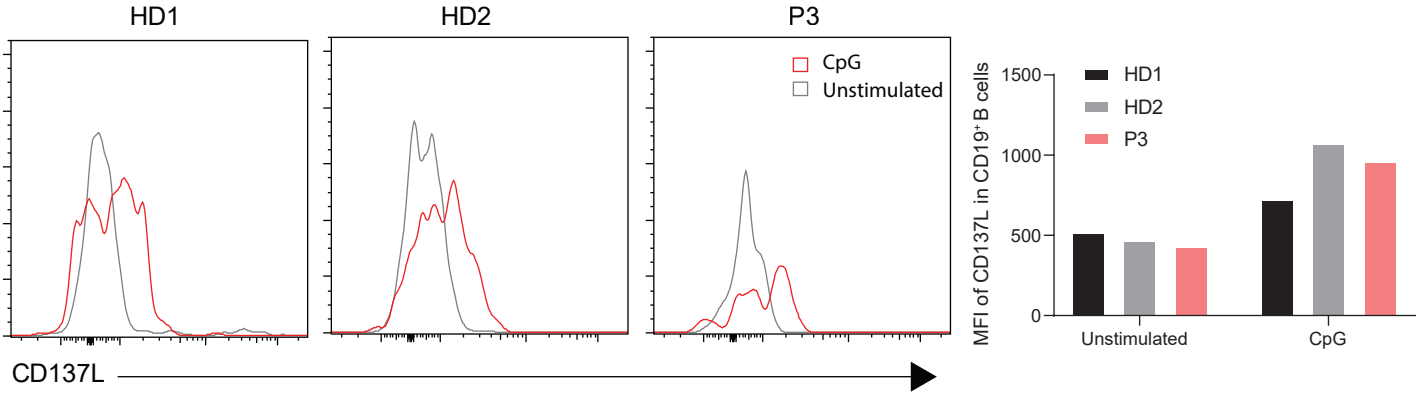

Supplementary Figure 10

A CD86 cell surface expression in sorted naive B-cell

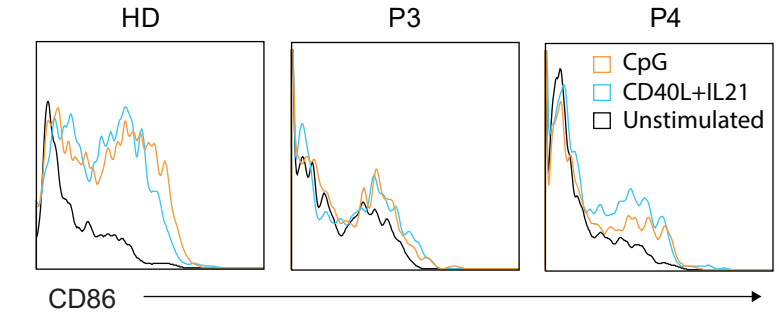

B Sorted naive B-cell proliferation

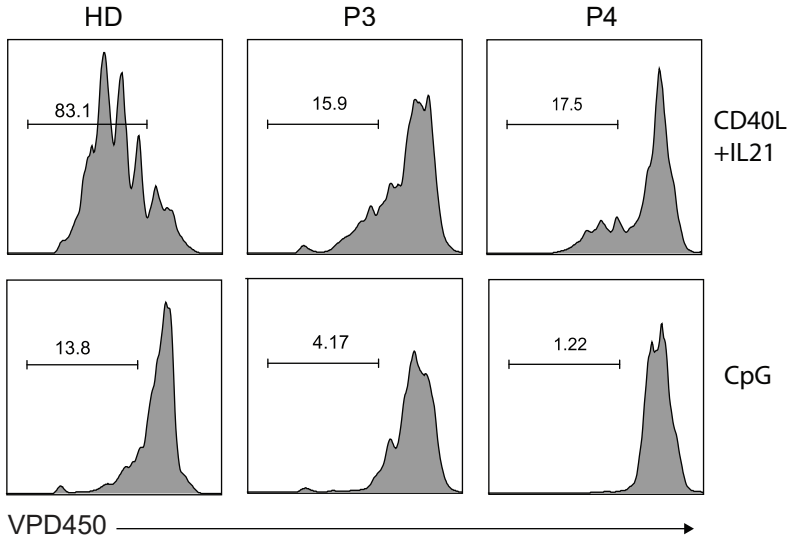

C Class switch recombination in sorted naive B-cells

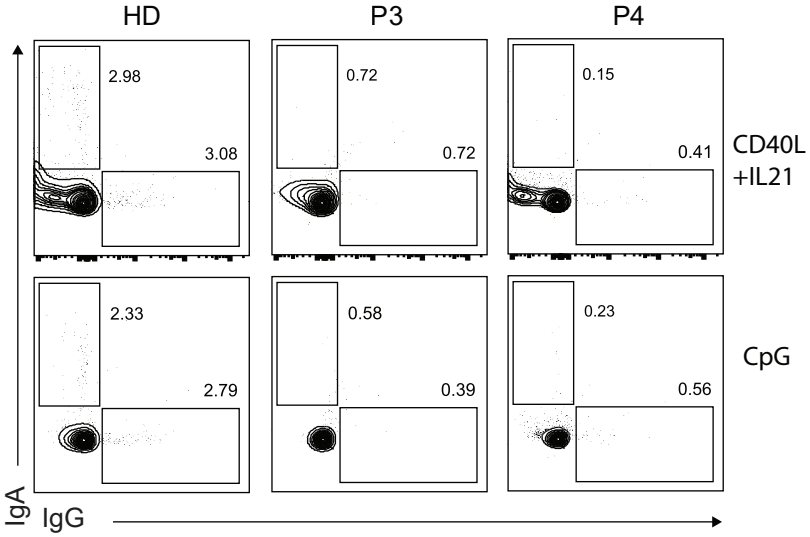

D CpG stimulation in sorted naive B-cells